Bioorganic Chemistry 78 (2018) 130–140

Contents lists available at ScienceDirect

Bioorganic Chemistry

journal homepage: www.elsevier.com/locate/bioorg

Synthesis and biological evaluation of pyrimidine bridged combretastatin derivatives as potential anticancer agents and mechanistic studies

Bhupinder Kumar [a], Praveen Sharma [b], Vivek Prakash Gupta [a], Madhu Khullar [c], Sandeep Singh [b], Nilambra Dogra [c,*], Vinod Kumar [a,*]

[a] Laboratory of Organic and Medicinal Chemistry, Department of Pharmaceutical Sciences and Natural Products, Central University of Punjab, Bathinda, Punjab 151001, India
[b] Laboratory of Molecular Medicine, Department of Human Genetics and Molecular Medicines, Central University of Punjab, Bathinda, Punjab 151001, India
[c] Department of Experimental Medicine and Biotechnology, PGIMER, Chandigarh 160012, India

ARTICLE INFO

Article history:
Received 23 January 2018
Revised 24 February 2018
Accepted 26 February 2018
Available online 28 February 2018

Keywords:
Pyrimidine
Combretastatin derivatives
Apoptosis
Tubulin inhibitors
Colchicine binding site
Anticancer

ABSTRACT

A number of pyrimidine bridged combretastatin derivatives were designed, synthesized and evaluated for anticancer activities against breast cancer (MCF-7) and lung cancer (A549) cell lines using MTT assays. Most of the synthesized compounds displayed good anticancer activity with IC_{50} values in low micromolar range. Compounds **4a** and **4p** were found most potent in the series with IC_{50} values of 4.67 μM & 3.38 μM and 4.63 μM & 3.71 μM against MCF7 and A549 cancer cell lines, respectively. Biological evaluation of these compounds showed that selective cancer cell toxicity (*in vitro* using human lung and breast cancer cell lines) might be due to the inhibition of antioxidant enzymes instigating elevated ROS levels which triggers intrinsic apoptotic pathways. These compounds were found nontoxic to the normal human primary cells. Compound **4a**, was found to be competitive inhibitor of colchicine and in the tubulin binding assay it showed tubulin polymerization inhibition potential comparable to colchicine. The molecular modeling studies also showed that the synthesized compounds fit well in the colchicine-binding pocket.

1. Introduction

Cancer is a multifactorial disease and considered as the most serious health problem all over the world. Despite recent advances in our understanding of the biological processes leading to the development of cancer, there is still need for the development of more potent and effective anticancer agents for the complete eradication of the disease [1]. Multi-drug resistance and acute toxicity are the two major issues with most of the currently available chemotherapeutic agents [2,3]. Therefore, novel anticancer agents need to be developed that are more potent, safe and selective. In a quest for the discovery of more effective anticancer drugs, a large number of structurally diverse synthetic and natural products have been screened for their anticancer potential [4,5]. Microtubules have been explored as an important target for the anticancer drug development. Microtubules play crucial role in the spindle formation during cell-division. A highly dynamic equilibrium exists between the microtubules and the free tubulin dimers [4]. Any disruption in the dynamic equilibrium of tubulin-microtubule blocks cell-division at the metaphase–anaphase transition that leads to the induction of the mitochondrial apoptosis [6].

Numerous structurally different natural as well as synthetic compounds have been identified that target microtubule polymerization [7]. Since last few years combretastatins have received special attention due to their simple structure and easy synthesis [8,9]. Combretastatin A-4 (CA-4) binds with the colchicine binding site and disrupts microtubule polymerization and induces rapid vascular disruption which leads to tumor cell death [10,11]. Fosbretabulin, a water-soluble phosphate prodrug of CA-4, is under phase II/III clinical trials alone and/or in combination with other chemotherapeutic agents. Although, numerous CA-4 analogs have been developed with improved antitubulin activities, but clinical application of these agents is not successful till now [12]. Thus, it is a challenge to synthesize CA-4 analogs with improved activity along with therapeutic potency.

* Corresponding authors at: Laboratory of Organic and Medicinal Chemistry, Department of Pharmaceutical Sciences and Natural Products, Central University of Punjab, Bathinda, Punjab 151001, India (V. Kumar). Department of Experimental Medicine and Biotechnology, PGIMER, Chandigarh 160012, India (N. Dogra).
E-mail addresses: nilambra@gmail.com (N. Dogra), vinod.kumar@cup.edu.in (V. Kumar).

https://doi.org/10.1016/j.bioorg.2018.02.027
0045-2068/

Most of the combretastatin derivatives have been synthesized by carrying out modifications at the ring A and ring B. In addition, olefinic bond of combretastatins have been replaced with number of heterocyclic rings such as, thiazole [13], tetrazole, triazoles [14,15], imidazole [16], pyrazole [17], Oxazole [18], pyrrole [19], indole, furan [20], benzene, pyridine [21], pyrimidine [22], quinoline, isoquinoline, isoxazole, thiazoline, pyrazoline, thiophene [23], benzofuran [24] etc. Many of these compounds displayed cytotoxic and antitubulin activities. In combretastatins, a two carbon olefinic bridge and *cis* conformation was considered crucial for the cytotoxicity and antitubulin activity of the compounds. However, a number of other compounds with varying length of linker chain between the two phenyl rings have been reported with antitubulin activity. For example, phenstatin, with a carbonyl group in place of double bond displayed antitubulin activity [25]. Likewise, chalcone with a three carbon chain, strongly inhibit tubulin polymerization with improved cytotoxicity [26]. In the present study, we have designed, synthesized and evaluated a new series of pyrimidine bridged combretastatin derivatives for their anticancer activities.

Different compounds with a core pyrimidine ring have been reported as inhibitors of cyclin-dependent kinases (CDK) [27], tumor necrosis factor R (TNF-R) [28], ableson protein tyrosine kinase (Abl) [29], 3-phosphatidylinositol kinases (PI-3 K) [30], protein kinase B (Aktkinase), and cytokines [31]. Gangjee et al. synthesized two series of the compounds based on the 6-CH_3 cyclopenta [d]pyrimidine and pyrrolo[2,3-d]pyrimidine scaffolds. These compounds displayed potent antiproliferative activity at nanomolar concentration and target the colchicine binding site of tubulin [32]. Xie et al. synthesized 2,4,5-substituted pyrimidine derivatives and evaluated for antiproliferative and anti-tubulin activities. These compounds arrested cell cycle at G2/M phases of the cell cycle (EC_{50} = 20 nM) and were found as competitive inhibitors of the colchicine binding site [31]. Zhang et al. synthesized a series of 4-substituted 2,6-dimethylfuro[2,3-d]pyrimidines as dual inhibitors of the microtubules and tyrosine kinases (RTKs). These compounds exhibited microtubules de-polymerization activity with EC_{50} values in nano molar range [22]. Zheng et al. evaluated anticancer activities of 3-carbon and 4-carbon linker analogous of combretastatin-A4. 3-Carbon linkers with bridged pyridine ring showed better activities as compared to 4-carbon linkers and a non-heterocyclic bridged system [21].

In the current studies, we have introduced a pyrimidine ring as a 3-carbon linker between the two phenyl rings (Fig. 1) to maintain the *cis* locked conformation of combretastatin-A4. Ring A and ring B were optionally substituted with different substituents having electron releasing and electron withdrawing effects. Molecular modeling studies were also performed in order to understand the binding interactions of the synthesized compounds with tubulin proteins. The mechanistic studies revealed that this series of compounds displayed anticancer activity through inhibition of antioxidant enzymes which may destabilizes the mitochondrial membrane and trigger intrinsic apoptotic pathway. Further, colchicine site binding agents arrest the cell cycle at G2/M phase that lead to mitochondrial apoptosis [6].

2. Results and discussion

2.1. Chemistry

Target compounds were synthesized as described in Scheme 1. The intermediate chalcones were synthesized through Aldol condensation. Aldehydes **(1)** and acetophenones **(2)** were condensed to give 1,3-Diphenyl-2-propen-1-one **(chalcones, 3)** in varying yields, and recrystallized to obtain pure products. These intermediate chalcones **(3)** were further reacted with acetamidine/formamidine/guanidine to give corresponding pyrimidine bridged analogous of combretastatins **(4a-4t)**. All the synthesized compounds were characterized by ^{1}H NMR, ^{13}C NMR and ESI-MS.

2.2. Biological evaluation of compounds and discussion

2.2.1. Synthesized compounds exhibited significant cytotoxicity and selectively against cancer cell lines

All the synthesized compounds **(4a-4t)** were investigated for their *in vitro* cytotoxicity against human MCF-7 (breast cancer) and A549 (lung cancer) cancer cell lines using standard MTT assays (Table 1 and supplementary Fig. S1a and S1b) while colchicine was used as a reference compound. Three different concentrations (1 μM, 5 μM, and 25 μM in triplicate) of the compounds were used and the results were analyzed after 48 h of drug treatment. It has been found that compound **4a-4c, 4e, 4f, 4j, 4m-4p** showed better antiproliferative activities as compared to the reference colchicine against both the cell lines. In this series of compounds, **4a** and **4p** showed best antiproliferative activity against both the cancer cell lines. Compound **4a** displayed IC_{50} values of 4.67 μM and 3.38 μM while **4p** showed IC_{50} values of 4.63 μM and 3.71 μM against MCF-7 and A549 cell lines, respectively (48 h post treatment). These compounds were also tested on human peripheral blood cells (hPBMCs) which represented the normal cell types. The results indicated that this series of compounds did not display cytotoxicity against the tested cells up to 5 μM concentration of the test drugs. Thus, this series of compounds can selectively target cancer cells and can be used as lead for the development of effective anticancer drug (supplementary information Fig. S1a and S1b).

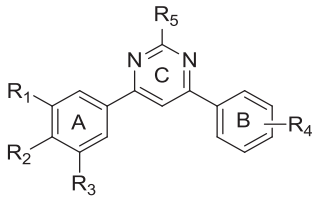

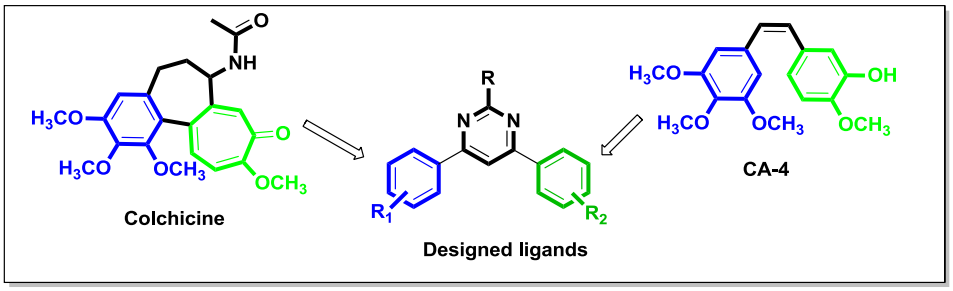

Fig. 1. Target compounds and their structural comparison with colchicine and combretastatin (CA-4).

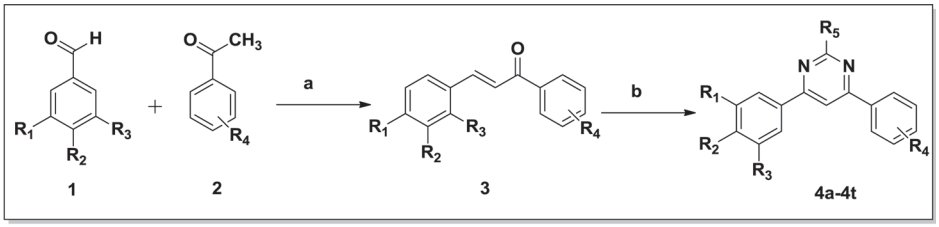

Reagent and conditions: a) 10%NaOH in H_2O, MeOH, strring, rt **b)** Acetamidine/formamidine/guanidine (1.2 eq), anhyd Na_2CO_3 (2.4eq), acetonitrile (10ml) , reflux,

Scheme 1. Synthesis of pyrimidine bridged analogs of combretastatins.

Table 1
In vitro antiproliferative activity (IC_{50} in μM) of compounds **4a to 4t** against MCF-7 and A549 cancer cell lines.

Compound	R_1	R_2	R_3	R_4	R_5	MCF-7 (μM)	A549 (μM)
4a	–H	–H	–H	H	$-CH_3$	4.67 ± 0.16	3.38 ± 0.29
4b	–H	–H	–H	*p*-OCH_3	$-CH_3$	4.78 ± 0.33	3.41 ± 0.54
4c	$-OCH_3$	$-OCH_3$	–H	H	$-CH_3$	7.95 ± 0.51	4.8 ± 0.14
4d	$-OCH_3$	$-OCH_3$	$-OCH_3$	*p*-OCH_3	$-CH_3$	16.49 ± 0.65	>25
4e	–H	$-OCH_3$	–H	H	–H	5.98 ± 0.41	3.16 ± 0.33
4f	–H	–H	–H	H	–H	4.88 ± 0.21	3.17 ± 0.68
4g	$-OCH_3$	$-OCH_3$	$-OCH_3$	*p*-Cl	$-CH_3$	11.01 ± 0.27	>25
4h	$-OCH_3$	$-OCH_3$	$-OCH_3$	H	$-CH_3$	>25	>25
4i	$-OCH_3$	$-OCH_3$	$-OCH_3$	*p*-CH_3	$-CH_3$	20.58 ± 1.58	>25
4j	$-OCH_3$	$-OCH_3$	–H	*p*-CH_3	$-CH_3$	4.89 ± 0.57	3.37 ± 0.39
4k	$-OCH_3$	$-OCH_3$	–H	*p*-OCH_3	$-CH_3$	>25	>25
4l	–H	–H	–H	H	$-NH_2$	10.84 ± 0.57	>25
4m	–H	$-OCH_3$	–H	H	$-NH_2$	4.93 ± 0.46	4.85 ± 0.41
4n	$-OCH_3$	$-OCH_3$	$-OCH_3$	*p*-OCH_3	$-NH_2$	4.85 ± 0.33	5.91 ± 0.52
4o	$-OCH_3$	$-OCH_3$	–H	*p*-Cl	$-NH_2$	5.10 ± 0.93	4.23 ± 0.43
4p	$-OCH_3$	$-OCH_3$	$-OCH_3$	2,4-Cl	$-NH_2$	4.63 ± 0.87	3.71 ± 0.21
4q	$-OCH_3$	$-OCH_3$	$-OCH_3$	*p*-CH_3	$-NH_2$	19.37 ± 0.85	>25
4r	$-OCH_3$	$-OCH_3$	$-OCH_3$	–Ph	$-NH_2$	>25	>25
4s	$-OCH_3$	$-OCH_3$	$-OCH_3$	*p*-Cl	$-NH_2$	>25	>25
4t	$-OCH_3$	$-OCH_3$	$-OCH_3$	H	$-NH_2$	>25	>25
Colchicine						5.13 ± 0.35	5.19 ± 0.42

2.3. The anticancer activity of synthesized compounds is via induction of apoptosis

Compounds **4a** and **4p** showed significant activity against the tested human cancer cell lines and hence, these were selected for further mechanistic investigations. Compounds **4a**, **4b**, and **4f** are least substituted compounds while **4p** is highly substituted compound. Hence, out of the least substituted compound, **4a** was selected and **4p** was picked from highly substituted derivatives as most potent compounds for cell line studies. In order to understand the mechanism of cell death induced by compounds **4a** and **4p**, a cytofluorimetric analysis was performed at A549 cancer cell lines using Muse™ Annexin V and Dead Cell kit to detect the phosphatidyl serine membrane translocation. This is considered as a major hallmark of late stage apoptosis. A549 human cancer cell lines were treated (24 h) with **4a, 4p** and colchicine as reference compound at 5 μM concentrations. It has been found that compounds **4a** and **4p** caused apoptotic cell death up to 64.10% and 44.34% while colchicine showed cell death up to 49.72% as compared to the control experiments (73.58% live cells). Hence, from these results it can be concluded that the primary mode of cell death with the tested compounds is through apoptosis (see Fig. 2).

2.4. Compounds induce apoptosis via deregulation of antioxidant defense system

Mitochondrial changes including variations in the mitochondrial membrane potential ($\Delta\Psi_m$), are the key events during drug-induced apoptosis [33]. If mitochondrial membrane potential is altered, it leads to leakage of cytochrome-c into the cytoplasm which triggers the intrinsic apoptotic pathway. Thus, to understand the mode of apoptosis, we analyzed mitochondrial membrane potential ($\Delta\Psi_m$), using a fluorescence probe, JC-1 (5,5′,6,6′-Tetrachloro-1,1′,3,3′-tetraethylbenzimidazolcarbocyanine) which has been shown to be more specific for mitochondria than for other fluorescent dyes such as $DiOC_6(3)$ or rhodamine 123. In normal state, mitochondria with normal $\Delta\Psi_m$, JC-1 is aggregated (red/orange fluorescence), while in mitochondria with depolarization, JC-1 forms monomers (green fluorescence). Thus, A549 cancer cells were treated with the synthesized compounds at the 5 μM and 25 μM concentrations. Compounds **4a, 4c**, **4e, 4f, 4m, 4o** and colchicine caused destabilization of the mitochondrial membrane at 5 μM concentration (Fig. 3) whereas compound **4b, 4c**, **4e, 4n and 4p** were more active at 25 μM concentration. It has been observed that there were significant alterations in the mitochondrial membrane potential upon drug treatment which indicated that the intrinsic pathway of apoptosis (mitochondrial mediated) might be responsible for the selective cancer cell apoptosis.

Major modulators of intrinsic pathway are mostly internal signaling cascades and free radicals are known to be one of the most important modulator. Thus, we further hypothesized that the alterations of antioxidant defense system of the cells might be responsible for the mitochondrial membrane potential alterations. In order to test the hypothesis, we measured the impact of selected compounds (**4a** and **4p**) *in vitro,* in three enzymes namely super oxide dismutase (SOD), catalase and glutathione reductase which are involved in the free radical detoxification. Superoxide dismutase enzyme catalyzes the dismutation of superoxide radical

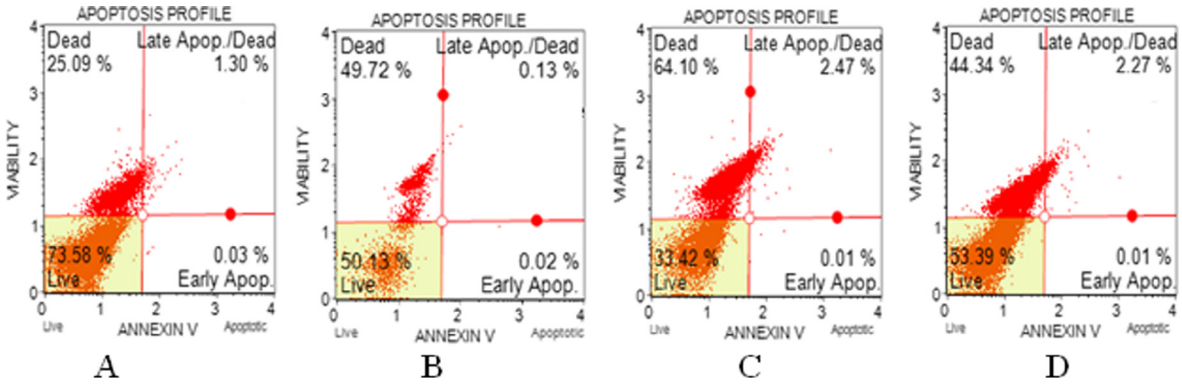

Fig. 2. Apoptosis effect on human A549 cell line induced by compound (A) control, (B) colchicine (5 μM), (C) **4a** (5 μM) and (D) **4p** (5 μM). The lower left quadrants represent live cells, the lower right quadrants are for early/primary apoptotic cells, upper right quadrants are for late/secondary apoptotic cells, while the upper left quadrants represent cells damaged during the procedure.

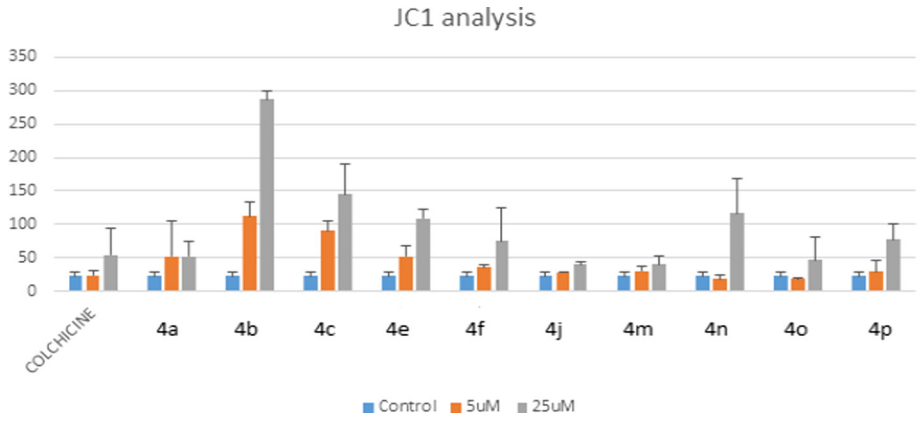

Fig. 3. Treatment of A549 cancer cells with selected compounds and their JC1 analysis showing variations in the mitochondrial membrane potential ($\Delta\Psi_m$).

$(O_2)^{2-}$ into oxygen and hydrogen peroxide. Thereafter, catalase converts the hydrogen peroxide into oxygen and water. Thus, these enzymes are responsible for the antioxidant defense in almost all the cells. It has been found that there was no significant change in SOD activity (Fig. 4a) while catalase and glutathione reductase activities were reduced significantly upon treatment with compounds **4a** and **4p** (Fig. 4b and 4c).

Glutathione plays crucial role in the DNA synthesis by maintaining reduced levels of glutaredoxin or thioredoxin. In addition, a direct correlation has been observed between glutathione levels and cell proliferation. Moreover, we performed *in vitro* DPPH assay and found that the compounds have no antioxidant property of their own (supplementary information Fig. S2, results not shown). Collectively these results indicated that the compounds are able to disturb the cellular antioxidant defense system, which in-turn, lead to elevated intracellular ROS, and triggers intrinsic apoptotic pathway.

2.5. Tubulin polymerization inhibition

This series of compounds are expected to mimic combretastatins and chalcones for their antitubulin activity. Hence, tubulin binding efficiency of these compounds was evaluated by an *in vitro* tubulin polymerization assay. Purified bovine tubulin was incubated with 10 μM **4a**, **4j**, **4o** or **4p**, and tubulin polymerization was recorded over time. Although all the four compounds showed inhibition of tubulin polymerization as compared to control, compound **4a** showed an inhibition comparable to colchicine which was used as a positive control (Fig. 5).

2.6. Competitive colchicine binding site assay

An *in vitro* competitive colchicine binding assay was performed in order to verify whether the compounds bind to the colchicine binding site of the tubulin. It has been found that addition of compound **4a** showed reduced fluorescence of the tubulin-colchicine complex. From these results it can be concluded that compound **4a** displaces colchicine from the tubulin-colchicine complex (Fig. 6). Thus, compound **4a** was found to be competitive inhibitor of colchicine.

2.7. Docking studies

From the literature search it was evident that most of the combretastatins and their derivatives bind to the colchicine binding site of the tubulin and inhibit tubulin polymerization [34,35]. The compounds **4a** and **4p** displayed good anticancer activities. These compounds were docked into the active site of the tubulin (PDB entry: 4O2B) to explore their interactions with the colchicine binding site and to investigate their binding pattern (Fig. 7). The interactions between the ligands and receptor site were scored using Glide (GLIDE 11.1 module of Schrödinger Suite). Validation of the docking protocol was done by re-docking of colchicine into the crystal structure of tubulin. In the validation results, it has been found that compounds **4a** and **4p** occupy the same binding pocket as done by colchicine. The root-mean square deviation (RMSD) of docked colchicine to the co-crystallized ligand was found to be 0.224 Å, displaying good reproducibility of the ligand binding mode. Both the compounds fit well in the colchicine binding site

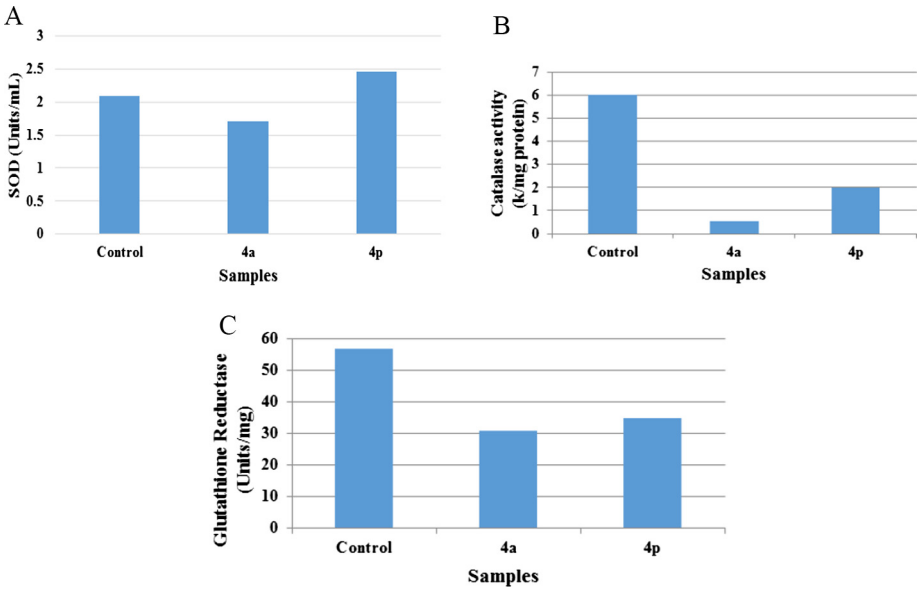

Fig. 4. Impact of **4a** and **4p** on (a) super oxide dismutase (SOD) activity, (b) catalase activity and (c) glutathione reductase activity.

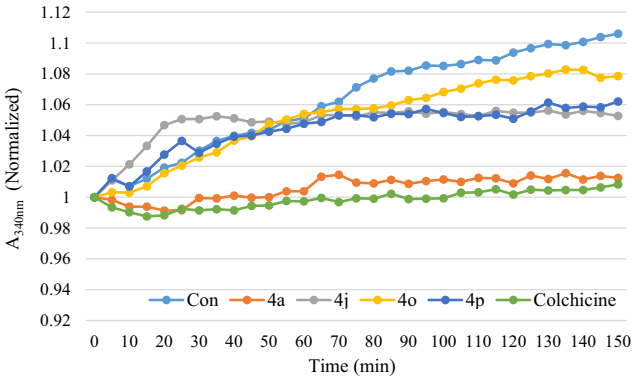

Fig. 5. *In vitro* studies of compounds **4a**, **4j**, **4o** and **4p** for their tubulin polymerization inhibition.

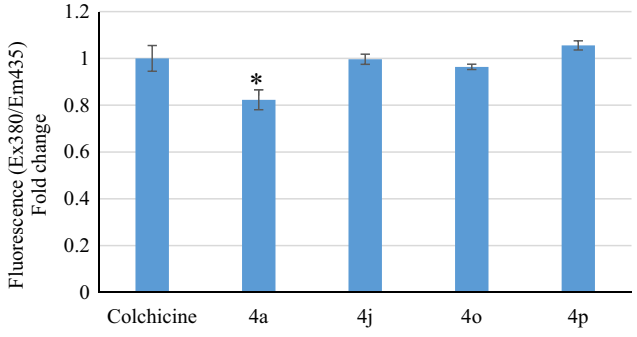

Fig. 6. Binding of **4a**, **4j**, **4o** and **4p** on colchicine binding site of tubulin determined by competitive colchicine binding assay.

and presence of the pyrimidine ring showed extended interaction pattern.

Interestingly, docking poses of the **4p** showed that trimethoxy substituents in ring A were oriented towards α-tubulin while trimethoxy groups in colchicine were directed toward β-tubulin (Fig. 7). Colchicine forms hydrogen bond through its carbonyl oxygen present in the ring with Val-181 residue of α-tubulin while most of its structural part fit inside the hydrophobic pocket of β-tubulin formed by Leu-242, Leu-248, Ala-250, Leu-252 and Leu-255 residues. On the other hand, trimethoxy substituents of compound **4p** were exposed to α-tubulin residues Ser-178, Thr-179 and Ala-180 and $-NH_2$ group present on the pyrimidine ring form hydrogen bonds with Ala-317 and Lys-352 residues of β-tubulin. Phenyl ring with dichloro substitutions and pyrimidine ring fit well in the hydrophobic pocket of colchicine binding site of tubulin formed by Ile-318, Leu-242, Leu-248, Ala-250, Leu-252, Leu-255 and Ile-378 of β-tubulin. These findings suggest that the synthesized pyrimidine bridged derivatives of combretastatins might act as dual site inhibitors of α- and β-tubulin complexes and their cytotoxicity could be due to the dual inhibition of α- and β-tubulin heterodimer.

Further these compounds were docked into the active site of the tubulin (PDB entry: 5LYJ) to explore their interactions with the combretastatin binding site and to investigate their binding pattern (Fig. 8). In the validation results, it has been found that compounds **4a** and **4p** bind to the same binding pocket as done by combretastatin. Combretastatin forms hydrogen bond through its hydroxy group present in the ring with Thr-179 residue of α-tubulin while trimethoxy ring of its structural part fit inside the hydrophobic pocket of β-tubulin formed by Leu-242, Leu-248, Ala-250, Leu-255, Ala-316, Ala-317, Ile-318 and Ile-378 residues. Similarly, in case of compound **4p,** $-NH_2$ group present at pyrimidine ring forms the hydrogen bond with Thr-179 residue of α-tubulin while trimethoxy ring of its structural part fit inside the hydrophobic pocket of β-tubulin formed by Leu-242, Leu-248, Ala-250, Leu-255, Ala-316, Ala-317, Ile-318 and Ile-378 residues. It showed additional π-π interactions with Lys-352 residue of β-tubulin due to presence of pyrimidine ring. Thus, it can be concluded that the introduction of pyrimidine ring as C3 linker between two phenyl rings improve the interaction at the combretastatin binding site.

2.8. ADME studies

ADME studies were performed to investigate the physicochemical properties of the synthesized compounds. In order to analyze the drug like characteristics of the compounds, these were evaluated for different parameters as described by Lipinski's rule of five

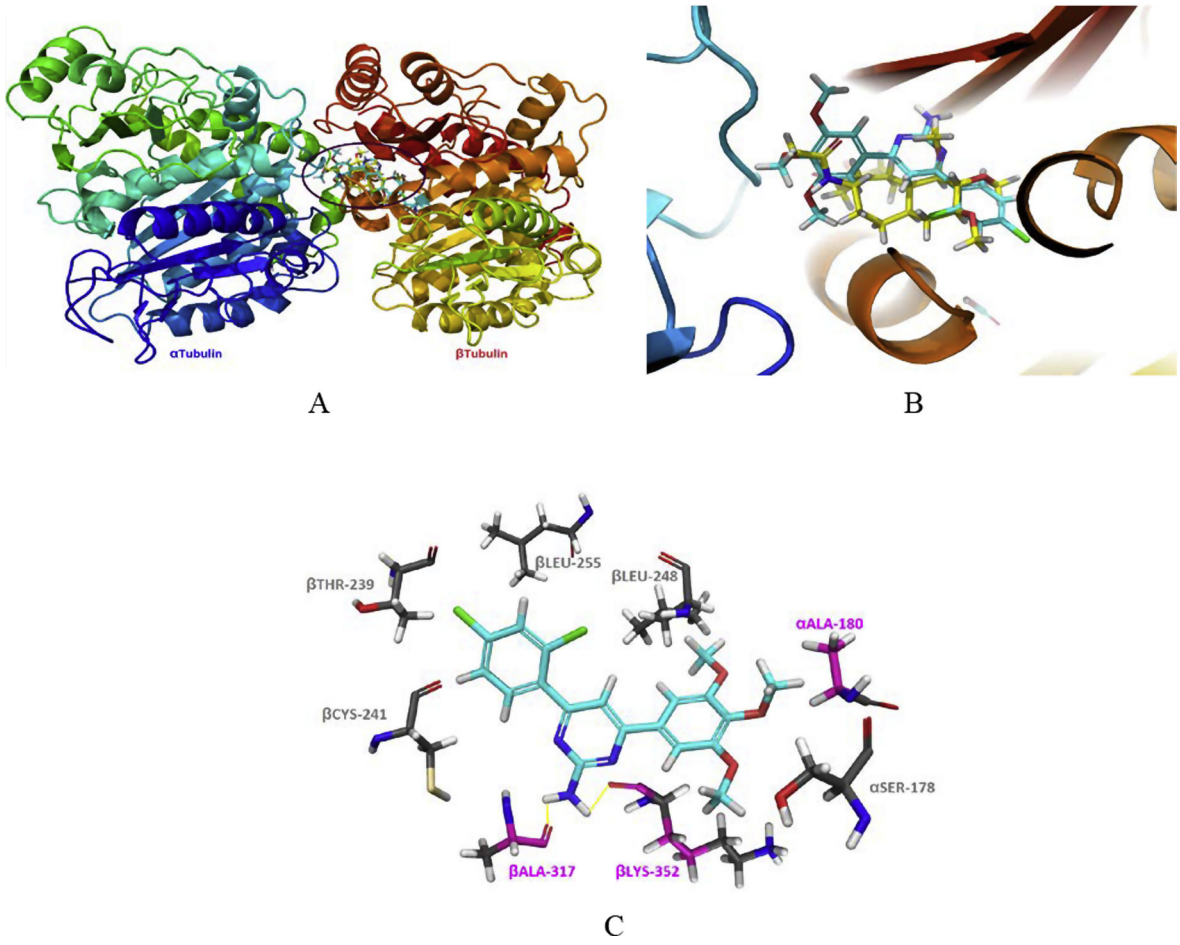

Fig. 7. (A) overlapping of compound **4p** (cyan) with colchicine (yellow) at colchicine binding site between α- and β–tubulin, (B) close view of the overlapped compound **4p** (cyan) with colchicine (yellow) at the colchicine binding site and (C) interactions of **4p** at the hydrophobic pocket of colchicine binding site (Yellow line shows hydrogen bonding) with various amino acid residues of the α- and β–tubulin. (For interpretation of the references to colour in this figure legend, the reader is referred to the web version of this article.)

using qikprop application of Schrodinger. The optimum Log P (<5) value is an important physiochemical property indicating the lipophilicity and the ability of the molecule to cross various biological membranes. The compounds **4a** and **4p** displayed lipophilicity within the range of 4.46 to 4.62. Number of hydrogen bond donors and hydrogen bond acceptors also lies within the range and molecular weight of the synthesized compounds were also less than 500 (Table 2). The compound with low dipole moment was found more efficiently binding to the colchicine binding site and have higher cytotoxic potential. Compound **4p** also showed less number of metabolic reactions (3) as compared to the standard tubulin inhibitors colchicine (5) and combretastatin (5). Most importantly, **4a** and **4p** showed 100% human oral absorption. Thus, it can be concluded that the compounds with high lipophilicity and low dipole moment exhibit good drug like characteristics.

2.9. SAR studies

In the current study, different optionally substituted pyrimidine bridged combretastatin derivatives have been synthesized and evaluated. Acetamidine, formadine and guanidine were used for the synthesis of pyrimidine ring and to keep the phenyl rings in *cis* locked confirmation. Most of the compounds displayed anticancer activities against MCF7 and A549 cancer cell lines in low micromolar range. In general, it has been observed that unsubstituted or monosubstituted compounds (**4a**, **4b**, **4e**, **4f** and **4m**) were more active as compared to the di and tri substituted derivatives (Table 1). Most of the trimethoxy substituted derivatives (**4d**, **4h**, **4i**, **4r**, **4s** and **4t**) were found 3–5-fold less active except compound **4n** and **4p**. Compound 4n with trimethoxy substitution on ring A and 4-methoxy substitution on ring B showed IC_{50} values of 4.85 μM and 5.91 μM against MCF7 and A549 cancer cell lines, respectively. However, compound **4p** with a 2,4-dichloro substitution on ring B was found most potent in the series with IC_{50} values of 4.63 μM and 3.71 μM against MCF7 and A549 cancer cell lines, respectively. Similarly, compound **4a** was also found effective against both the cancer cell lines with IC_{50} values of 4.67 μM (MCF7) and 3.38 μM (A549). There was no significant effect on the activity when CH_3, H and NH_2 groups were interchanged on the pyrimidine ring (**4b**, **4e** and **4m**). Replacement of electron releasing methyl group in ring B (**4i**) with electron withdrawing chloro group (**4g**) increased the activity by almost twofold. In contrast, compound with a para methyl substitution on ring B (**4j**) was 5-fold more active than corresponding para methoxy derivative (**4k**). Replacement of ring B by a naphthyl ring (**4r**) decreases the activity, might be due to increase in the lipophilicity (higher Log P) of the compound. Unsubstituted derivative with no substituent on any of the three rings also showed good anticancer activity with IC_{50} values of 4.88 μM and 3.17 μM against MCF7 and A549 cancer cell lines, respectively.

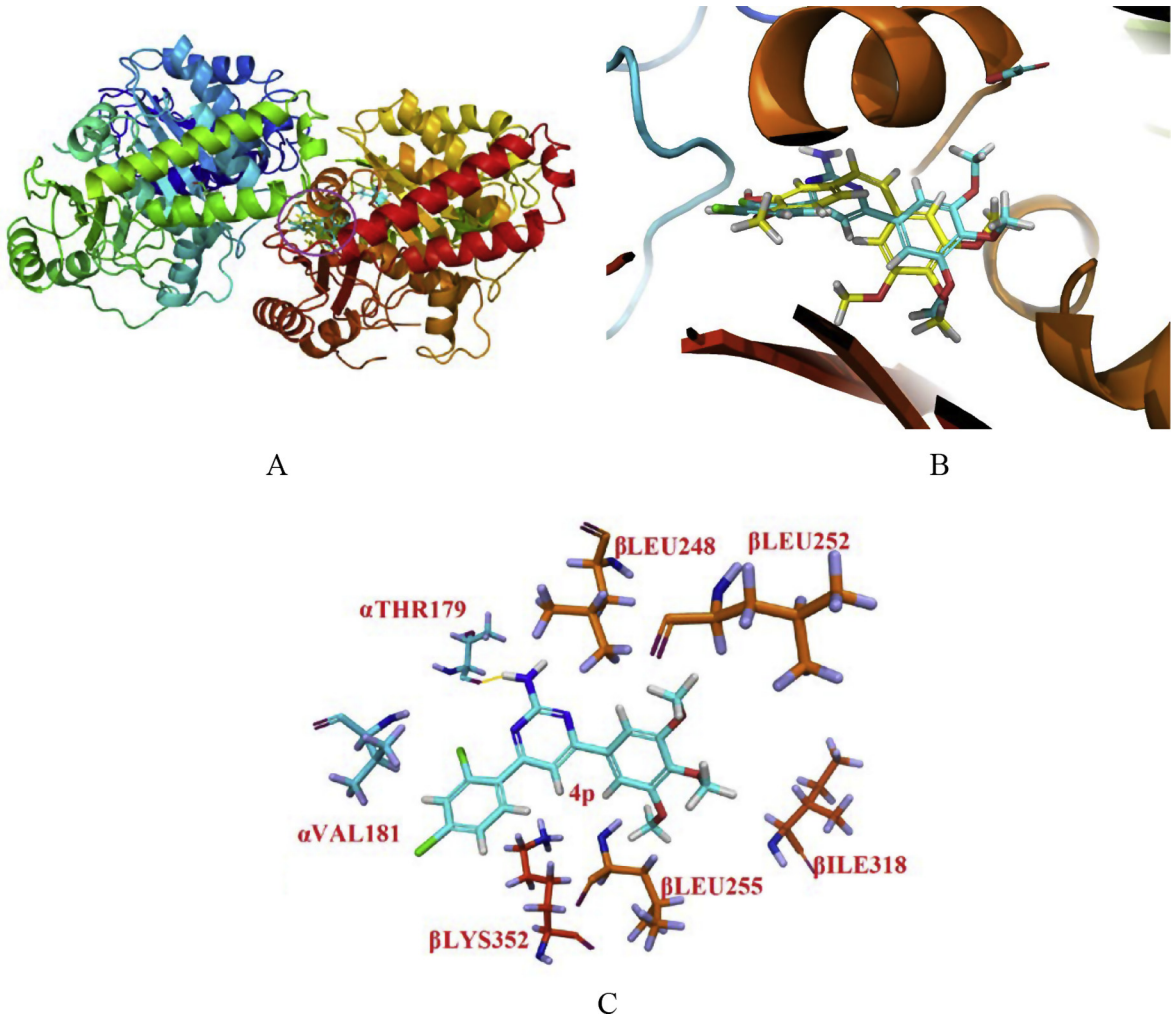

Fig. 8. (A) overlapping of compound **4p** (cyan) with combretastatin (yellow) at combretastatin binding site between α- and β–tubulin, (B) close view of the overlapped compound **4p** (cyan) with combretastatin (yellow) at the colchicine binding site and (C) interactions of **4p** at the hydrophobic pocket of combretastatin binding site (Yellow line shows hydrogen bonding) with various amino acid residues of the α- and β–tubulin. (For interpretation of the references to colour in this figure legend, the reader is referred to the web version of this article.)

Table 2
Drug like characteristics of compounds **4a** and **4p** as determined by qikprop application of Schrodinger.

Name	Mol. Wt.	Log P	HB donor	HB acceptor	% Human oral absorption	Dipole	#metb
4a	246.311	4.465	0	2	100	1.95	1
4p	406.268	4.629	2	5	100	1.48	3
Colchicine	399.443	2.704	1	8	95.43	6.91	5
Combretastatin	316.353	4.045	1	4	100	4.02	5

3. Conclusion

Twenty pyrimidine bridged combretastatin derivatives (**4a**-**4t**) have been synthesized and evaluated for anticancer activities against MCF7 and A549 cancer cell lines. Most of the compounds displayed anticancer activities in low micromolar range and some of the compounds in this series were found even better as compared to the reference colchicine. Compounds **4a** and **4p** were found most active in this series and hence various mechanistic studies were performed on these compounds. It has been observed that compounds **4a** and **4p** inhibit the cell proliferation of cancer cells by inducing apoptosis. JC-1 analysis showed this series of compounds alter the mitochondrial membrane potential which leads to leakage of cytochrome-c into the cytoplasm triggering intrinsic apoptotic pathway. Further investigations on the antioxidant defense system of the cells revealed that treatment of compounds **4a** and **4p** did not produce any change in SOD activity however, catalase and glutathione reductase activities were reduced significantly. In the competitive tubulin binding assay, it has been found that compound **4a** binds to the tubulin at the colchicine binding site. The docking studies of compounds **4a** and **4p** showed that these compounds fit well in the colchicine binding site of the tubulin. Further, the tested compounds inhibited tubulin polymerization and compound **4a** showed significant inhibition potential comparable to colchicine. Collectively, it can be concluded that the synthesized compounds might be able to deregulate multiple pathways to induce cancer cell specific apoptosis (colchicine like action as well as modulation of intrinsic apoptotic pathway).

4. Experimental

4.1. General

All the reagents were of AR/GR quality and purchased from Sigma-Aldrich, Loba-Chemie Pvt. Ltd., S.D. Fine Chemicals, Spectrochem, Sisco Research Laboratory and Avra Synthesis Ltd. and were used without further purification. The progress of the reaction was monitored by TLC using petroleum ether/ethyl acetate and chloroform/methanol as the mobile phase on pre-coated Merck TLC plates & glass plates made of F254 UV grade silica in JSGW UV/fluorescent analysis cabinet and/or iodine chamber. Melting points were recorded on the Stuart melting point apparatus (SMP-30) with open glass capillary tubed. Infrared (IR) spectra of compounds were recorded with KBr on a Bruker FT-IR spectrophotometer. ^{1}H and ^{13}C Nuclear magnetic resonance (NMR) spectra was obtained in $CDCl_3$/d6-DMSO on a Bruker Avance II (400 MHz) NMR spectrometer using TMS (δ = 0) as internal standard at Panjab University, Chandigarh. Mass spectra were recorded in Shimazdu GC–MS (ESI), Central University of Punjab, Bathinda, Punjab, India.

4.2. General procedure for synthesis of 3

The mixture of benzaldehyde **1** (2g), acetophenone **2** (1eq), sodium hydroxide (10% in water, 5 eq) in methanol (15 ml) was stirred at room temperature until completion of the reaction**.** The product formation was monitored by TLC. After complete product formation, the reaction mixture was evaporated at rota-evaporator. Water was added to the residue and the precipitated product was filtered. dried and recrystallized in the methanol.

4.3. General procedure for synthesis of 4a-4t

The mixture of the chalcone **3** (0.2 g), amidine (1.2 eq), and sodium carbonate (2.4 eq) in acetonitrile (10 ml) was refluxed for overnight at 80 °C. The time required for the product formation varies from different products (24-48hrs). The progress of reaction was monitored by the TLC in 30% ethylacetate/petroleum ether. After the completion of the reaction, the reaction mixture was dried on the rotavapor. To the residue water was added and crude product was extracted with with ethyl acetate. The organic portion was separated and washed with water, brine, dried over anhydrous sodium sulfate and rota-evaporated. Compounds were purified through column chromatography using chloroform and methanol as solvent. Final product formation was confirmed by EI-MS, CHN and HRMS.

2-methyl-4,6-diphenylpyrimidine (4a): yield 85%, light yellow solid, **^{1}H NMR** (400 MHz, $CDCl_3$, TMS = 0) 2.87 (3H, s), 7.51–7.53 (6H, m), 7.89 (1H, s), 8.11–8.14 (4H, m), **^{13}C NMR:** (100 MHz, $CDCl_3$, TMS = 0) δ: 168.68, 164.99, 137.60, 130.76, 129.066, 127.36, 110.24, 26.64. HRMS: m/z $[M+H]^+$ for $C_{17}H_{14}N_2$, calculated 247.1235; observed: 247.1215.

4-(4-methoxyphenyl)-2-methyl-6-phenylpyrimidine (4b): [36] yield 78%, white solid, **^{1}H NMR** (400 MHz, $CDCl_3$, TMS = 0) 2.84 (3H, s), 3.88 (3H, s), 7.02 (2H, d, J = 8 Hz), 7.50–7.52 (3H, m), 7.82 (1H, s), 8.10–8.12 (4H, m), **^{13}C NMR:** (100 MHz, $CDCl_3$, TMS = 0) δ: 168.51, 164.74, 164.39, 161.90, 137.79, 130.62, 129.94, 129.02, 128.85, 128.68, 127.33, 114.37, 109.34, 55.54, 26.64. MS-EI: m/z $[M]^+$ for $C_{18}H_{16}N_2O$, calculated 276.13; observed: 276, **CHN:** calculated C- 78.24, H-5.84, N-10.14, observed C- 78.98, H-5.68, N-10.49.

4-(3,4-dimethoxyphenyl)-2-methyl-6-phenylpyrimidine (4c): yield 73%, cream solid, **^{1}H NMR** (400 MHz, $CDCl_3$, TMS = 0) 2.85 (3H, s), 3.95 (3H, s), 4.02 (3H, s), 6.97 (1H, d, J = 8 Hz), 7.49–7.53 (3H, m), 7.67–7.69 (1H, m), 7.77 (1H, d, J = 1.96 Hz), 7.82 (1H, s), 8.09–8.12 (2H, m), **^{13}C NMR:** (100 MHz, $CDCl_3$, TMS = 0) δ: 168.42, 164.67, 164.31, 151.36, 149.37, 137.61, 130.55, 130.19, 128.93, 127.25, 120.28, 111.02, 109.98, 109.40, 56.08, 56.03, 26.53. HRMS: m/z $[M+H]^+$ for $C_{19}H_{18}N_2O_2$, calculated 307.1447; observed: 307.1438.

4-(4-methoxyphenyl)-2-methyl-6-(3,4,5-trimethoxyphenyl) pyrimidine (4d): yield 72%, light brown solid, **^{1}H NMR** (400 MHz, $CDCl_3$, TMS = 0) 2.83 (3H, s), 3.88 (3H, s), 3.92 (3H, s), 3.99 (6H, s), 7.04 (2H, d, J = 7 Hz), 7.33 (2H, s), 7.73 (1H, s), 8.11 (2H, d, J = 7 Hz) **^{13}C NMR:** (100 MHz, CDCl3, TMS = 0) δ: 168.33, 164.32, 164.31, 161.84, 153.61, 140.31, 133.23, 129.85, 128.77, 114.29, 109.02, 104.50, 61.01, 56.36, 55.45, 26.51. HRMS: m/z $[M+H]^+$ for $C_{21}H_{22}N_2O_2$, calculated 367.1658; observed: 366.1644.

4-(4-methoxyphenyl)-6-phenylpyrimidine (4e): yield 74%, off white solid, **^{1}H NMR** (400 MHz, $CDCl_3$, TMS = 0) 3.88 (3H, s), 7.02 (2H, dd), 7.51–7.54 (3H, m), 8.03 (1H, s), 8.10–8.14 (4H, m), 9.26 (1H, s) **^{13}C NMR:** (100 MHz, $CDCl_3$, TMS = 0) δ: 164.45, 164.18, 162.06, 159.11, 137.21, 130.84, 129.36, 129.02, 128.74, 127.18, 114.39, 111.98, 55.47. MS-EI: m/z $[M]^+$ for $C_{17}H_{14}N_2O$, calculated 262.11; observed: 262, **CHN:** calculated C- 77.84, H-5.38, N-10.68, observed C- 77.37, H-5.29, N-10.87.

4,6-diphenylpyrimidine (4f):[37,38] yield 75%, off white solid, **^{1}H NMR** (400 MHz, $CDCl_3$, TMS = 0) 7.50–7.56 (6H, m), 8.09 (1H, s), 8.11–8.16 (4H, m), 9.31 (1H, s), **^{13}C NMR:** (100 MHz, $CDCl_3$, TMS = 0) δ: 164.73, 159.22, 137.03, 130.99, 129.07, 127.22, 112.89. HRMS: m/z $[M+H]^+$ for $C_{16}H_{12}N_2$, calculated 233.1079; observed: 233.1067.

4-(4-chlorophenyl)-2-methyl-6-(3,4,5-trimethoxyphenyl)pyrimidine (4g): yield 82%, off yellow solid, **^{1}H NMR** (400 MHz, $CDCl_3$, TMS = 0) 2.77 (3H, s), 3.85 (3H, s), 3.92 (6H, s), 7.27 (2H, s), 7.43 (2H, d, J = 8 Hz), 7.69 (1H, s), 8.01 (2H, d, J = 8 Hz) **^{13}C NMR:** (100 MHz, $CDCl_3$, TMS = 0) δ: 167.57, 163.70, 162.57, 152.64, 139.60, 135.88, 134.89, 131.79, 128.15, 127.54, 108.49, 103.60, 59.98, 55.37, 28.68, 25.43. MS-EI: m/z $[M]^+$ for $C_{20}H_{19}ClN_2O_3$, calculated 370.11; observed: 370, **CHN:** calculated C- 64.78, H-5.16, N-7.55, observed C- 64.03, H-5.05, N-7.47.

2-methyl-4-phenyl-6-(3,4,5-trimethoxyphenyl)pyrimidine (4h): yield 84%, light brown solid, **^{1}H NMR** (400 MHz, $CDCl_3$, TMS = 0) 2.86 (3H, s), 3.92 (3H, s), 3.99 (6H, s), 7.36 (2H, s), 7.51–7.53 (3H, m), 7.80 (1H, s), 8.10–8.13 (2H, m) **^{13}C NMR:** (100 MHz, $CDCl_3$, TMS = 0) δ: 168.50, 164.92, 164.51, 153.65, 140.50, 137.55, 133.00, 130.66, 128.96, 127.28, 109.88, 104.59, 61.00, 56.38, 26.50. MS-EI: m/z $[M]^+$ for $C_{20}H_{20}N_2O_3$, calculated 336.15; observed: 336, **CHN:** calculated C- 71.41, H-5.99, N-8.33, observed C- 72.00, H-6.27, N-8.33.

2-methyl-4-(p-tolyl)-6-(3,4,5-trimethoxyphenyl)pyrimidine (4i): yield 81%, light yellow solid, **^{1}H NMR** (400 MHz, $CDCl_3$, TMS = 0) 2.43 (3H, s), 2.84 (3H, s), 3.92 (3H, s), 3.99 (6H, s), 7.26–7.34 (4H, m), 7.77 (1H, s), 8.01 (2H, d, J = 8 Hz) **^{13}C NMR:** (100 MHz, $CDCl_3$, TMS = 0) δ: 168.41, 164.82, 164.40, 153.63, 141.03, 140.42, 134.68, 133.14, 129.67, 127.17, 109.53, 104.58, 60.99, 56.38, 26.50, 21.46. MS-EI: m/z $[M]^+$ for $C_{21}H_{22}N_2O_3$, calculated 350.16; observed: 350, **CHN:** calculated C- 71.98, H-6.33, N-7.99, observed C- 71.41, H-6.52, N-7.29.

4-(3,4-dimethoxyphenyl)-2-methyl-6-(p-tolyl)pyrimidine (4j): yield 79%, light yellow solid, **^{1}H NMR** (400 MHz, $CDCl_3$, TMS = 0) 2.42 (3H, s), 2.83 (3H, s), 3.95 (3H, s), 4.02 (3H, s), 6.98 (1H, d, J = 8 Hz), 7.32 (2H, d, J = 8 Hz), 7.66–7.68 (1H, m), 7.76 (1H, s), 7.79 (1H, s), 8.02 (2H, d, J = 8 Hz) **^{13}C NMR:** (100 MHz, $CDCl_3$, TMS = 0) δ: 168.33, 164.58, 164.19, 151.31, 149.37, 140.87, 134.81, 130.34, 129.64, 127.13, 120.24, 111.04, 110.04, 109.02, 56.08, 56.02, 26.53, 21.45. MS-EI: m/z $[M]^+$ for $C_{20}H_{20}N_2O_2$, calculated 320.15; observed: 320, **CHN:** calculated C- 74.98, H-6.29, N- 8.74, observed C- 75.30, H-6.57, N-8.31.

4-(3,4-dimethoxyphenyl)-6-(4-methoxyphenyl)-2-methylpyrimidine (4k):[36] yield 78%, off yellow solid, **^{1}H NMR** (400 MHz,

$CDCl_3$, TMS = 0) 2.82 (3H, s), 3.86 (3H, s), 3.96 (3H, s), 4.02 (3H, s), 6.99 (1H, d, J = 8 Hz), 7.03 (2H, d, J = 8 Hz), 7.65–7.68 (1H, m), 7.76 (2H, s), 8.09–8.11 (2H, m) **^{13}C NMR:** (100 MHz, $CDCl_3$, TMS = 0) δ: 168.27, 164.10, 161.75, 151.27, 149.36, 130.74, 130.42, 128.72, 120.21, 114.27, 113.80, 111.03, 110.03, 108.52, 56.08, 56.03, 55.44, 26.52. HRMS: m/z $[M+H]^+$ for $C_{20}H_{20}N_2O_3$, calculated 337.1552; observed: 337.1534.

4, 6-diphenylpyrimidin-2-amine (4l):[39] yield 53%, white solid, **^{1}H NMR** (400 MHz, $CDCl_3$, TMS = 0) 5.47 (2H, s), 7.45 (1H, s), 7.457.51 (6H, m), 8.04–8.06 (4H, m), **^{13}C NMR:** (100 MHz, $CDCl_3$, TMS = 0) δ: 166.36, 163.79, 137.85, 130.55, 128.88, 127.23, 104.42. MS-EI: m/z $[M]^+$ for $C_{16}H_{13}N_3$, calculated 247.11; observed: 247.

4-(4-methoxyphenyl)-6-phenylpyrimidin-2-amine (4m):[39] yield 55%, off white solid, **^{1}H NMR** (400 MHz, $CDCl_3$, TMS = 0) 3.87 (3H, s), 5.23 (2H, s), 7.01 (2H, d, J = 9.2 Hz), 7.41 (1H, s), 7.487.49 (3H, m), 8.02–8.05 (4H, m), **^{13}C NMR:** (100 MHz, $CDCl_3$, TMS = 0) δ: 166.11, 165.77, 163.60, 161.76, 138.03, 130.40, 128.88, 128.74, 127.21, 114.22, 103.69, 55.54. MS-EI: m/z $[M]^+$ for $C_{17}H_{15}N_3O$, calculated 277.12; observed: 277.

4-(4-methoxyphenyl)-6-(3, 4, 5-trimethoxyphenyl) pyrimidin-2-amine (4n):[40] yield 77%, light yellow solid, **^{1}H NMR** (400 MHz, $CDCl_3$, TMS = 0) 3.87 (3H, s), 3.91 (3H, s), 3.97 (6H, s), 5.27(2H, s), 7.02 (2H, d, J = 6.96 Hz), 7.28 (2H, s), 7.33 (1H, s), 8.04 (2H, d, J = 6.84 Hz), **^{13}C NMR:** (100 MHz, $CDCl_3$, TMS = 0) δ: 165.70, 165.61, 163.47, 161.69, 153.45, 140.13, 133.42, 130.07, 128.64, 114.12, 104.36, 103.29, 60.99, 56.32, 55.4. MS-EI: m/z $[M]^+$ for $C_{20}H_{21}N_3O_4$, calculated 367.15; observed: 367.

4-(4-chlorophenyl)-6-(3, 4-dimethoxyphenyl) pyrimidin-2-amine (4o): yield 64%, light brown solid, **^{1}H NMR** (400 MHz, $CDCl_3$, TMS = 0) 3.95 (3H, s), 4.00 (3H, s), 5.22 (2H, s), 6.96 (1H, d, J = 8.44 Hz), 7.37 (2H, s), 7.47 (2H, d, J = 6.72 Hz), 7.63 (1H, dd, J_1 = 8.4 Hz, J_2 = 2.04 Hz), 7.70 (1H, s), 8.00 (2H, d, J = 6.76 Hz), **^{13}C NMR:** (100 MHz, $CDCl_3$, TMS = 0) δ: 165.88, 164.67, 163.51, 151.33, 149.25, 136.51, 136.27, 130.23, 128.9, 128.41, 120.18, 110.90, 109.93, 103.29, 56.05, 56.0. MS-EI: m/z $[M]^+$ for $C_{18}H_{16}ClN_3O_2$, calculated 341.09; observed: 341.

4-(2, 4-dichlorophenyl)-6-(3, 4, 5-trimethoxyphenyl) pyrimidin-2-amine (4p): yield 70%, off yellow solid, **^{1}H NMR** (400 MHz, $CDCl_3$, TMS = 0) 3.91 (3H, s), 3.95 (6H, s), 5.32 (2H, s), 7.26–7.28 (1H, m), 7.39 (1H, dd, J_1 = 8.24 Hz, J_2 =1.96 Hz), 7.52 (1H, d, J = 2.04 Hz), 7.58 (1H, d, J = 8.32 Hz), **^{13}C NMR:** (100 MHz, $CDCl_3$, TMS = 0) δ: 165.29, 164.84, 163.29, 153.49, 140.46, 136.23, 135.76, 132.94, 132.63, 131.80, 130.14, 127.50, 108.20, 104.42, 61.00, 56.28 **CHN:** calculated C- 56.17, H-4.22, N-10.34, observed C- 56.18, H-4.57, N-9.34. MS-EI: m/z $[M]^+$ for $C_{19}H_{17}Cl_2N_3O_3$, calculated 405.06; observed: 405.

4-(p-tolyl)-6-(3, 4, 5-trimethoxyphenyl) pyrimidin-2-amine (4q): yield 68%, off white solid, **^{1}H NMR** (400 MHz, $CDCl_3$, TMS = 0) 2.42 (3H, s), 3.91 (3H, s), 3.97 (6H, s), 5.30 (2H, s), 7.26–7.31 (4H, m), 7.35 (1H, s), 7.96 (2H, d, J = 8.16 Hz), **^{13}C NMR:** (100 MHz, $CDCl_3$, TMS = 0) δ: 166.22, 165.73, 163.52, 153.46, 140.85, 140.16, 134.89, 133.36, 129.53, 127.05, 104.37, 103.80, 61.0, 56.32, 21.4. MS-EI: m/z $[M]^+$ for $C_{20}H_{21}N_3O_3$, calculated 351.16; observed: 351.

4-(naphthalen-2-yl)-6-(3, 4, 5-trimethoxyphenyl) pyrimidin-2-amine (4r): yield 72%, white solid, **^{1}H NMR** (400 MHz, $CDCl_3$, TMS = 0) 3.91 (3H, s), 3.94 (6H, s), 5.43 (2H, s), 7.25 (1H, s), 7.30 (2H, s), 7.49–7.53 (2H, m), 7.53–7.59 (1H, m), 7.65–7.67 (1H, m), 7.91–7.96 (2H, m), 8.15–8-8.18 (1H, m), **^{13}C NMR:** (100 MHz, $CDCl_3$, TMS = 0) δ: 168.48, 165.37, 163.27, 153.50, 140.36, 136.95, 133.88, 132.85, 130.61, 129.77, 128.50, 126.90, 126.80, 126.21, 125.39, 125.27, 108.61, 104.39, 61.00, 56.29, 50.73. MS-EI: m/z $[M]^+$ for $C_{23}H_{21}N_3O_3$, calculated 387.16; observed: 387, **CHN:** calculated C- 71.30, H-5.46, N-10.85, observed C- 71.39, H-5.27, N-10.56.

4-(4-chlorophenyl)-6-(3, 4, 5-trimethoxyphenyl) pyrimidin-2-amine (4s):[40] yield 67%, off yellow solid, **^{1}H NMR** (400 MHz, $CDCl_3$, TMS = 0) 3.80 (3H, s), 3.94 (6H, s), 6.43 (2H, s), 7.46 (2H, s), 7.51 (2H, d, J = 8.56 Hz), 7.60 (1H, s), 8.22 (1H, d, J = 8.6 Hz), **^{13}C NMR:** (100 MHz, $CDCl_3$, TMS = 0) δ: 164.77, 163.59, 163.54, 152.84, 139.51, 136.00, 135.33, 132.67, 128.50, 128.31, 104.24, 101.86, 60.06, 55.90. MS-EI: m/z $[M]^+$ for $C_{19}H_{18}ClN_3O_3$, calculated 371.10; observed: 371.

4-phenyl-6-(3, 4, 5-trimethoxyphenyl) pyrimidin-2-amine (4t): yield 58%, yellowish brown solid, **^{1}H NMR** (400 MHz, $CDCl_3$, TMS = 0) δ 3.91 (3H, s), 3.97 (6H, s), 5.31(2H, s), 7.30 (2H, s), 7.38 (1H, s), 7.49–7.51 (3H, m), 8.03–8.05 (2H, m), **^{13}C NMR:** (100 MHz, $CDCl_3$, TMS = 0) δ: 166.33, 165.86, 163.54, 153.48, 140.26, 137.77, 133.23, 130.51, 128.81, 127.51, 104.40, 104.10, 61.00, 56.33. MS-EI: m/z $[M]^+$ for $C_{19}H_{19}N_3O_3$, calculated 337.14; observed: 337, **CHN:** calculated C- 67.64, H-5.68, N-12.46, observed C- 67.13, H-5.41, N-12.66.

4.4. Biological studies

4.4.1. Cytotoxic studies

MTT is a colorimetric assay used for the measurement of cell proliferation. The tetrazolium yellow compound MTT (3-[4,5-dimethylthiazol-2-yl]-2,5- diphenyl tetrazolium bromide) is reduced to an insoluble purple coloured formazan product by mitochondrial reductase or succinate dehydrogenase in metabolically active cells only. When formazan passes to the mitochondria it gets solubilized with DMSO and measured spectrophotometrically.

To carry out the MTT assay, cell lines (MCF7) were grown in DMEM medium with 5 ml serum containing medium. Upon the 70–80% growth, the sub-culturing of cells was done. Cells were counted using automated cell counter. Nearly 8,000–10,000 cells were seeded in each well of the 96 well plates. The plate was incubated at 37 °C with 5% CO_2 for 24 h followed by serum starvation for 8hrs for synchronization and replenishing with complete media. The treatment was given to the cells in triplicate concentrations of 1 μM, 5 μM and 25 μM and incubated for 48 h. MTT solution (5 mg/10 ml) was added after removing the media from each well and incubated in the dark for 4 h. At the end of 4 h, the MTT solution was removed from each well and the intracellular precipitate was dissolved in DMSO solution and the absorbance of the violet color formed as consequence of DMSO addition, is read spectrometrically at 570 nm and expressed as % inhibition (Mean ± S.D).

4.4.2. Free radical scavenging assay (DPPH assay)

Tubes were filled with 3 ml methanol containing extracts inside it and then DPPH was added to test tubes (1 ml) in dark and kept for incubation for 30 min. The absorbance was measured at 517 nm on UV-Spectrophotometer.

4.4.3. Evaluation of antioxidant enzyme inhibition

4.4.3.1. Superoxide dismutase (SOD) inhibition assay. 1.5 ml of 0.1 M Tris HCl buffer was added to cuvette followed by 0.5 ml of 6 mM EDTA followed by 1 ml of 6 mM Pyrogallol solution and 0.1 ml of sample extract was added and then mixed properly and then absorbance was measured at 420 nm after intervals of 30 s on UV-spectrophotometer.

4.4.3.2. Catalase inhibition assay. In 900 μL of 50 mM sodium phosphate buffer, 0.1 ml of test compound and hydrogen peroxide was added. Decrease in absorbance was measured after intervals of 30 s for 3 min at 240 nm.

4.4.3.3. Glutathione reductase inhibition assay. Using UV-spectrophotometer, in a cuvette 0.945 ml PB_{200} followed by addition of 5 μL DTNB and 10 μL sample then NADPH was added. Rapidly GR enzyme was added and absorbance at 412 nm was recorded after intervals of 30 s. and then GSSG was added and again recorded in intervals of 30 s till 3 min.

4.4.4. JC1 analysis

In 96-well plate cancer cells were seeded with appropriate treatment. Then, after 24 h cells were washed with PBS and incubated with JC 1 for 30 min. Then, wash the cells to remove extra dye with 1x PBS, and then fluorescence was measured using Synergy H1 microplate reader (green monomers with Ex 485 nm/Em 535 nm and red J aggregate with Ex 560 nm/Em 595 nm).

4.4.5. Apoptosis analysis

Apoptosis utilising Muse™ Annexin V and Dead Cell kit (Catalogue No. 15-0180) was performed using Muse™ cell analyser. Cellular samples (A549 previously treated with compound **Cochicine, 4a and 4p** for 24 h) were prepared by the predefined protocol of Muse™ Annexin V and Dead Cell kit. The total cells and media were centrifuged at 1200 rpm for 5 min and washed with 1x PBS. 50 μL of kit reagent was added and incubated for 30 min at room temperature in dark before the analysis.

4.4.6. Tubulin polymerization assay

Polymerization of the bovine tubulin was measured according to Beyer et al. [41]. The indicated drugs were added in triplicate into the wells of a 96 well plate. Bovine tubulin (1.8 mg/mL; Sigma) was added to ice-cold polymerization buffer (PEM: 80 mM PIPES, 0.5 mM EGTA, 2 mM $MgCl_2$, 10% glycerol, and 1 mM GTP) and centrifuged at maximum speed in a microcentrifuge for 5 min at 4 °C. Supernatant (100 uL/well) was immediately added to wells of the 96-well plate containing the drugs or dimethyl sulfoxide control in PEM buffer. After addition of tubulin, the plate was immediately placed in a spectrophotometer, which was maintained at 37 °C, and the absorbance was measured at 340 nm every 5 min for 2.5 h.

4.4.7. Competitive tubulin binding assay

4a, **4j**, **4o** and **4p** (10 μM each) were co-incubated with 3 μM colchicine in tubulin polymerization buffer containing 3 μM tubulin at 37 °C for 60 min. After incubation, the fluorescence of tubulin- colchicine complex was measured by using Tecan multimode reader at excitation wavelength of 380 nm and emission wavelength of 435 nm. The raw fluorescence values were normalized by setting the fluorescence of 3 μM tubulin with 3 μM colchicine to 100%.

4.5. Docking studies

To determine the mode of interaction between synthesized ligands and tubulin docking studies were performed. 2D structure of chemicals was prepared in ChemBioDraw ultra 8.0 software and converted to 3D structures in ligand preparation application of Maestro 11.1 (Schrödinger) software. The X-ray crystal structure of tubulin (PDB ID: 4O2B) co-crystallized with colchicine [42] and co-crystallized with Combretastatin A4 (PDB ID: 5LYJ) [39] was downloaded from the Protein Data Bank (www.rcsb.org). Further modification for protein preparations such as polar hydrogen addition, addition of side chains, and removal of water molecules was performed by Maestro 11.1 software. All Synthesized ligands along with co-crystallized colchicine and combretastatin were docked into the binding site of tubulin using Maestro 11.1 software. All atoms within a 5 Å around the co-crystallized ligand in crystal coordinates of tubulin was chosen as binding site. For each compound, the top-score docking poses were chosen for final ligand-target interaction analysis employing XP interaction visualizer of Maestro 11.1 software. Validation of docking procedure was first evaluated by re-docking of co-crystalized ligands into the tubulin binding sites. Qikprop application of Schrodinger suit was used to determine the drug like and ADME properties of the compounds.

Acknowledgement

VK and SS are thankful to the SERB-Department of Science and Technology, New Delhi for the extramural financial support grant number EMR/2015/002339. The authors declare no potential conflicts of interest.

Appendix A. Supplementary material

Supplementary data associated with this article can be found, in the online version, at https://doi.org/10.1016/j.bioorg.2018.02.027.

References

[1] C. Avendaño, J.C. Menendez, Medicinal Chemistry of Anticancer Drugs, Elsevier, 2008.
[2] G.L. Patrick, An Introduction to Medicinal Chemistry, Oxford University Press, 2013.
[3] H. Singla, S. Kalra, P. Kheterpal, V. Kumar, A. Munshi, Role of genomic alterations in HER2 positive breast carcinoma: focus on susceptibility and trastuzumab-therapy, Curr. Cancer Drug Target 17 (2017) 344–356.
[4] B. Kumar, R. Kumar, I. Skvortsova, V. Kumar, Mechanisms of tubulin binding ligands to target cancer cells: updates on their therapeutic potential and clinical trials, Curr. Cancer Drug Target 17 (2017) 357–375.
[5] I.-I. Skvortsova, V. Kumar, Editorial: Recent trends in anticancer drug development: challenges and opportunities, Curr. Med. Chem. 24 (2017) 4727–4728.
[6] E. Pasquier, M. Kavallaris, Microtubules: a dynamic target in cancer therapy, IUBMB Life 60 (2008) 165–170.
[7] R. Cao, M. Liu, M. Yin, Q. Liu, Y. Wang, N. Huang, Discovery of novel tubulin inhibitors via structure-based hierarchical virtual screening, J. Chem. Inf. Model. 52 (2012) 2730–2740.
[8] M. Davydova, I. Sorokina, T. Tolstikova, V. Mamatyuk, D. Fadeev, S. Vasilevsky, Synthesis of new combretastatin A-4 analogues and study of their anti-inflammatory activity, Russ. J. Bioorg. Chem. 41 (2015) 70–76.
[9] B. Kumar, S. Singh, I. Skvortsova, V. Kumar, Promising targets in anti-cancer drug development: recent updates, Curr. Med. Chem. 24 (2017) 4729–4752.
[10] G.R. Pettit, C. Temple Jr, V. Narayanan, R. Varma, M. Simpson, M. Boyd, G. Rener, N. Bansal, Antineoplastic agents 322. Synthesis of combretastatin A-4 prodrugs, Anti-cancer Drug Des. 10 (1995) 299–309.
[11] D. Patterson, G. Rustin, Vascular damaging agents, Clin. Oncol. 19 (2007) 443–456.
[12] C.J. Mooney, G. Nagaiah, P. Fu, J.K. Wasman, M.M. Cooney, P.S. Savvides, J.A. Bokar, A. Dowlati, D. Wang, S.S. Agarwala, A phase II trial of fosbretabulin in advanced anaplastic thyroid carcinoma and correlation of baseline serum-soluble intracellular adhesion molecule-1 with outcome, Thyroid 19 (2009) 233–240.
[13] W. Li, Y. Lu, Z. Wang, J.T. Dalton, D.D. Miller, Synthesis and antiproliferative activity of thiazolidine analogs for melanoma, Bioorg. Med. Chem. Lett. 17 (2007) 4113–4117.
[14] H.N. Pati, M. Wicks, H.L. Holt Jr, R. LeBlanc, P. Weisbruch, L. Forrest, M. Lee, Synthesis and biological evaluation of cis-combretastatin analogs and their novel 1, 2, 3-triazole derivatives, Heterocycl. Commun. 11 (2005) 117–120.
[15] R. Kaur, A. Ranjan Dwivedi, B. Kumar, V. Kumar, Recent developments on 1, 2, 4-triazole nucleus in anticancer compounds: a review, Anti-Cancer Agents Med. Chem. 16 (2016) 465–489.
[16] F. Bellina, S. Cauteruccio, S. Monti, R. Rossi, Novel imidazole-based combretastatin A-4 analogues: evaluation of their in vitro antitumor activity and molecular modeling study of their binding to the colchicine site of tubulin, Bioorg. Med. Chem. Lett. 16 (2006) 5757–5762.
[17] D.V. Tsyganov, L.D. Konyushkin, I.B. Karmanova, S.I. Firgang, Y.A. Strelenko, M. N. Semenova, A.S. Kiselyov, V.V. Semenov, cis-Restricted 3-aminopyrazole analogues of combretastatins: synthesis from plant polyalkoxybenzenes and biological evaluation in the cytotoxicity and phenotypic sea urchin embryo assays, J. Nat. Prod. 76 (2013) 1485–1491.
[18] L. Wang, K.W. Woods, Q. Li, K.J. Barr, R.W. McCroskey, S.M. Hannick, L. Gherke, R.B. Credo, Y.-H. Hui, K. Marsh, Potent, orally active heterocycle-based combretastatin A-4 analogues: synthesis, structure-activity relationship, pharmacokinetics, and in vivo antitumor activity evaluation, J. Med. Chem. 45 (2002) 1697–1711.
[19] N.M. O'Boyle, L.M. Greene, O. Bergin, J.-B. Fichet, T. McCabe, D.G. Lloyd, D.M. Zisterer, M.J. Meegan, Synthesis, evaluation and structural studies of

antiproliferative tubulin-targeting azetidin-2-ones, Bioorg. Med. Chem. 19 (2011) 2306–2325.
[20] T. Pirali, S. Busacca, L. Beltrami, D. Imovilli, F. Pagliai, G. Miglio, A. Massarotti, L. Verotta, G.C. Tron, G. Sorba, Synthesis and cytotoxic evaluation of combretafurans, potential scaffolds for dual-action antitumoral agents, J. Med. Chem. 49 (2006) 5372–5376.
[21] S. Zheng, Q. Zhong, M. Mottamal, Q. Zhang, C. Zhang, E. LeMelle, H. McFerrin, G. Wang, Design, synthesis, and biological evaluation of novel pyridine-bridged analogues of combretastatin-A4 as anticancer agents, J. Med. Chem. 57 (2014) 3369–3381.
[22] X. Zhang, S. Raghavan, M. Ihnat, E. Hamel, C. Zammiello, A. Bastian, S.L. Mooberry, A. Gangjee, The design, synthesis and biological evaluation of conformationally restricted 4-substituted-2, 6-dimethylfuro [2, 3-d] pyrimidines as multi-targeted receptor tyrosine kinase and microtubule inhibitors as potential antitumor agents, Bioorg. Med. Chem. 23 (2015) 2408–2423.
[23] B.L. Flynn, G.P. Flynn, E. Hamel, M.K. Jung, The synthesis and tubulin binding activity of thiophene-based analogues of combretastatin A-4, Bioorg. Med. Chem. Lett. 11 (2001) 2341–2343.
[24] G.R. Pettit, M.R. Rhodes, D.L. Herald, E. Hamel, J.M. Schmidt, R.K. Pettit, Antineoplastic agents. 445. Synthesis and evaluation of structural modifications of (Z)-and (E)-combretastatin A-4 1, J. Med. Chem. 48 (2005) 4087–4099.
[25] G.R. Pettit, B. Toki, D.L. Herald, P. Verdier-Pinard, M.R. Boyd, E. Hamel, R.K. Pettit, Antineoplastic agents. 379. Synthesis of phenstatin phosphate1a, J. Med. Chem. 41 (1998) 1688–1695.
[26] S. Ducki, R. Forrest, J.A. Hadfield, A. Kendall, N.J. Lawrence, A.T. McGown, D. Rennison, Potent antimitotic and cell growth inhibitory properties of substituted chalcones, Bioorg. Med. Chem. Lett. 8 (1998) 1051–1056.
[27] S. Wang, C. Meades, G. Wood, A. Osnowski, S. Anderson, R. Yuill, M. Thomas, M. Mezna, W. Jackson, C. Midgley, 2-Anilino-4-(thiazol-5-yl) pyrimidine CDK inhibitors: synthesis, SAR analysis, X-ray crystallography, and biological activity, J. Med. Chem. 47 (2004) 1662–1675.
[28] T.A. Brugel, J.A. Maier, M.P. Clark, M. Sabat, A. Golebiowski, R.G. Bookland, M.J. Laufersweiler, S.K. Laughlin, J.C. VanRens, B. De, Development of N-2, 4-pyrimidine-N-phenyl-N′-phenyl ureas as inhibitors of tumor necrosis factor alpha (TNF-α) synthesis. Part 1, Bioorg. Med. Chem. Lett. 16 (2006) 3510–3513.
[29] J. Zimmermann, E. Buchdunger, H. Mett, T. Meyer, N.B. Lydon, Potent and selective inhibitors of the Abl-kinase: phenylamino-pyrimidine (PAP) derivatives, Bioorg. Med. Chem. Lett. 7 (1997) 187–192.
[30] S. Pecchi, P.A. Renhowe, C. Taylor, S. Kaufman, H. Merritt, M. Wiesmann, K.R. Shoemaker, M.S. Knapp, E. Ornelas, T.F. Hendrickson, Identification and structure–activity relationship of 2-morpholino 6-(3-hydroxyphenyl) pyrimidines, a class of potent and selective PI3 kinase inhibitors, Bioorg. Med. Chem. Lett. 20 (2010) 6895–6898.
[31] F. Xie, H. Zhao, D. Li, H. Chen, H. Quan, X. Shi, L. Lou, Y. Hu, Synthesis and biological evaluation of 2, 4, 5-substituted pyrimidines as a new class of tubulin polymerization inhibitors, J. Med. Chem. 54 (2011) 3200–3205.
[32] A. Gangjee, Y. Zhao, L. Lin, S. Raghavan, E.G. Roberts, A.L. Risinger, E. Hamel, S.L. Mooberry, Synthesis and discovery of water-soluble microtubule targeting agents that bind to the colchicine site on tubulin and circumvent Pgp mediated resistance, J. Med. Chem. 53 (2010) 8116–8128.
[33] J. Kluza, P. Marchetti, M.-A. Gallego, S. Lancel, C. Fournier, A. Loyens, J.-C. Beauvillain, C. Bailly, Mitochondrial proliferation during apoptosis induced by anticancer agents: effects of doxorubicin and mitoxantrone on cancer and cardiac cells, Oncogene 23 (2004) 7018–7030.
[34] S. Ducki, Antimitotic chalcones and related compounds as inhibitors of tubulin assembly, Anti-Cancer Agents Med. Chem. 9 (2009) 336–347.
[35] N. Zhang, S. Ayral-Kaloustian, T. Nguyen, J. Afragola, R. Hernandez, J. Lucas, J. Gibbons, C. Beyer, Synthesis and SAR of [1, 2, 4] triazolo [1, 5-a] pyrimidines, a class of anticancer agents with a unique mechanism of tubulin inhibition, J. Med. Chem. 50 (2007) 319–327.
[36] L. Rong, H. Han, H. Jiang, Y. Dai, M. Zhuang, M. Cao, S. Tu, An efficient and convenient multicomponent reaction for the synthesis of 2-methyl-4, 6-diarylpyrimidine under solvent-free conditions, J. Heterocyclic Chem. 46 (2009) 890–894.
[37] E. Ivanova, M. Puzyk, K. Balashev, Cyclopalladated ethylenediamine complexes on the basis of 4-phenylpyrimidine and 4, 6-diphenylpyrimidine, Russ. J. Gen. Chem. 78 (2008) 1236–1240.
[38] F.-L. Qing, R. Wang, B. Li, X. Zheng, W.-D. Meng, Synthesis of 4, 6-disubstituted pyrimidines via Suzuki and Kumada coupling reaction of 4, 6-dichloropyrimidine, J. Fluorine Chem. 120 (2003) 21–24.
[39] N.D. Thanh, N.T. Thanh Mai, N.P. Nhan, Synthesis of some 2-amino-4, 6-diarylpyrimidine derivatives using microwave-assisted method, V. J. Chem. 47 (2014) 628.
[40] V. Pathak, H.K. Maurya, S. Sharma, K.K. Srivastava, A. Gupta, Synthesis and biological evaluation of substituted 4, 6-diarylpyrimidines and 3, 5-diphenyl-4, 5-dihydro-1H-pyrazoles as anti-tubercular agents, Bioorg. Med. Chem. Lett. 24 (2014) 2892–2896.
[41] C.F. Beyer, N. Zhang, R. Hernandez, D. Vitale, J. Lucas, T. Nguyen, C. Discafani, S. Ayral-Kaloustian, J.J. Gibbons, TTI-237: a novel microtubule-active compound with in vivo antitumor activity, Cancer Res. 68 (2008) 2292–2300.
[42] A.E. Prota, F. Danel, F. Bachmann, K. Bargsten, R.M. Buey, J. Pohlmann, S. Reinelt, H. Lane, M.O. Steinmetz, The novel microtubule-destabilizing drug BAL27862 binds to the colchicine site of tubulin with distinct effects on microtubule organization, J. Mol. Biol. 426 (2014) 1848–1860.